International Journal of Sciences and Techniques of Automatic control & computer engineering
IJ-STA, Volume 4, N° 2, December 2010, pp. 1388–1401.

Design of an Electrical Syringe Pump Using a Linear Tubular Step Actuator

Imen Saidi[1], Lilia El Amraoui Ouni[1, 2] and Mohamed Benrejeb[1]

[1] Unité de Recherche LARA Automatique, Ecole Nationale d'Ingénieurs de Tunis, B.P.37, Le Belvédère, 1002, Tunis.
[2] Ecole Supérieure de Technologie et d'Informatique, 45 rue des entrepreneurs Charguia 2, 2035 Tunis-Charthage

imen.saidi@gmail.com, lilia.elamraoui@enit.rnu.tn
mohamed.benrejeb@enit.rnu.tn

Abstract. *In this paper is developed an analytical model for design of a linear step actuator, dedicated to the motorization of a syringe pump used for the perfusion of a real incompressible drug. The chosen geometric parameters of the designed actuator are validated by the numerical finite element method.*

Keywords. *Design Syringe pump, Perfusion, Real incompressible drug, Linear step actuator, Finite element method, Geometrical parameters of the actuator.*

1. Introduction

The electric syringe pump allows to inject in slow and continues way medicamentous solution for therapeutic or diagnostic purpose. They also allow to transfuse blood components, such as, plasma, plates, globular concentrate [1].

In the case of cardiovascular and neurological diseases for example, the treatment by intravenous injection of solution for long duration, with adjustable flow and precise rate [1], requires programmable automatic syringes, able to be connected to a central network of monitoring.

These electric syringe pumps are generally designed around rotary actuator systems [2]. However linear actuators are able to develop direct linear movements with high dynamic and without rotary. However linear actuators are able to develop direct linear movements with high dynamic and without rotary to linear movement transform systems.

This paper was recommended for publication in revised form by the editor Staff.
Edition: CPU of Tunis, Tunisia, ISSN: 1737-7749

The actuator of motorization of the syringe pumps is dimensioned by taking account simultaneously of several physical phenomena present within the actuator constituting a multidisciplinary model of dimensioning. It elaborate via methods analytical and semi-analytical is composed of several models interacting between them representing an each particular physical phenomenon. It is broken up into five models: a magnetic model is obviously the base of the operation of the actuator; this one is strongly coupled by a thermal model making it possible to determine the heating of the actuator. To those, come to be added a mechanical model and a model of load, as well as an electric model.

In this direction, we are interested by the design of a linear step actuator for the motorization of a syringe pump for laminar flow incompressible drug perfusion. This actuator must be able to develop a linear incremental movement by steps of 1mm and a starting force is 2.5 Newton on each step displacement and a useful race of 100 mm.

Indeed, two methods are proposed for the design of this actuator, an analytical step one allowing the geometrical characteristics of the prototype determination, and a numerical using the finite element method which is a powerful tool in the field of the electromagnetic structural design, to validate the choice of the actuator design parameters.

2. Presentation of the electrical syringe pump

The Electric Syringe Pump (PSE) is an injection or perfusion apparatus. It is used when the patient is unable to swallow oral preparations, or when his general state does not allow him a normal catch of drugs. The principal vessels used for the perfusion are peripheral veins and central veins [1]. The injection flow of the drug can vary from 0.1 ml/h to 99.99 ml/h [2]; volumes of the most usually used syringes are 5 ml, 10 ml, 20 ml, 30 ml and 50 to 60 ml.

The electric syringe pump combines mechanical, electric and electronic parts. The mechanical part is used as support for the various types of syringes. It includes sensors which allow to check the fixing position of the piston. The piston of the PSE is directly coupled with the motorization system, which pushes the syringe contents towards the patient. This mechanical part is driven by a linear tubular step actuator. It presents four statoric phases and a toothed stator and plunger structure with the same tooth and slot widths. Non-magnetic separations are set between the statoric phases so that only one statoric phase can be aligned with plunger teeth when it is supplied. Fig.1. shows the global structure of the linear tubular actuator.

Finally the electronic controls the flows, the pressures and also the alarm manage.

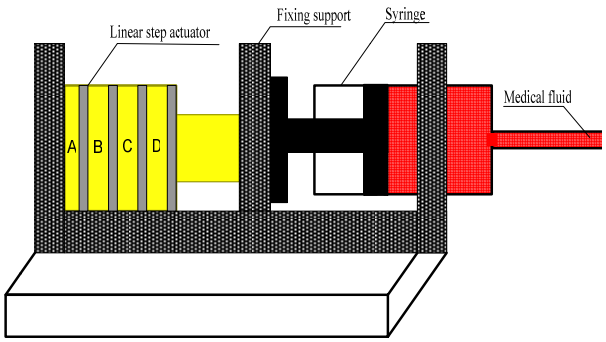

Fig. 1. Synoptic of the electric syringe pump

3. Design Considerations

The designed actuator must develop the axial force required to control the piston of the syringe in the presence of the aqueous solution to perfuse. Indeed, geometrical, mechanical, electric and electromagnetic performances depend on the axial force to produce. Thus it is necessary characterize the thrust force necessary to the piston displacement.

3.1. Modeling of thrust force

The modeling of the load force exerted on the piston of the syringe, Fig. 2. , is done under these assumptions:

- fluid in the syringe is incompressible;
- fluid in the syringe is in steady laminar flow state;
- no slip between the fluid and the syringe nor the needle walls;
- Internal diameter of the syringe greater than that of the needle.

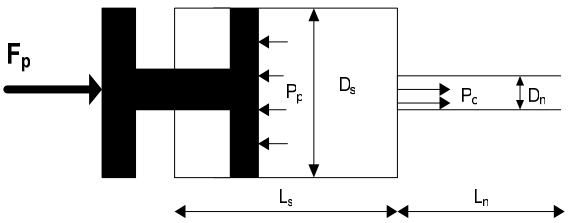

Fig.2. Synoptic description of the syringe

The expression of the thrust force F_p is given by the following equation:

$$F_p = PS_s \,. \tag{1}$$

where P is the pressure exerted on the piston and S_S the syringe section given by:

$$S_s = \frac{\Pi D_s^2}{4} \,. \tag{2}$$

where D_s is the internal diameter of the syringe.

The expression of the pressure P modeling the piston balance at constant speed is given by the following equation:

$$P = P_p + P_M - P_o \,. \tag{3}$$

where P_p is the fluid pressure at the piston, P_M the muscular pressure and P_o the fluid pressure at the needle exit.

From equations "(1)", "(2)" and "(3)" it comes:

$$F_p = \left(P_p + P_M - P_o\right)\left(\frac{\Pi D_s^2}{4}\right). \tag{4}$$

The energy balance of the system is deduced from the generalized Bernoulli equation, described by [3]:

$$\frac{P_p}{\rho} + (L_s - L_n)g + \frac{1}{2}\frac{V_1^2}{\alpha_1} = \frac{P_o}{\rho} + \frac{1}{2}\frac{V_2^2}{\alpha_2} + \sum F \,. \tag{5}$$

where V_1, V_2 are the average velocities respectively in the syringe and the needle, α_1 the kinetic energy correction factor at the air–fluid interface, α_2 the kinetic energy correction factor at the exit of the needle, g the gravity acceleration, ρ the fluid density, L_s the length of the syringe, L_n the length of the needle, and $\sum F$ is the sum of all friction losses between the air–fluid interface and the exit of the needle.

The average velocity V_1 approximately equals to zero, then the term $V_1^2/(2\alpha_1)$ can be neglected and the syringe pump is maintained horizontal, thus,

$$(L_s - L_n)g = 0 \,. \tag{6}$$

The friction losses $\sum F$ are predominantly those when associated with flowing in the needle [3] are given by:

$$\sum F = \frac{\Delta P}{\rho} + K_c \frac{V_2^2}{2} \,. \tag{7}$$

where ΔP is the frictional pressure drop through the needle, K_c the loss correction factor. The major losses are modeled by the first term, and the second models term minor losses.
From equations "(4)", "(5)" and "(6)" it comes:

$$P_p = P_o + \frac{1}{2}\rho\frac{V_2^2}{\alpha_2} + \Delta P + \frac{1}{2}\rho K_c V_2^2 . \quad (8)$$

In the case of Newtonian fluids, α has the value of 0.5 and K_c is suggested to be 0.23.

The flow rate of fluid in the needle is considered as a fully developed laminar flow of Newtonian fluid. So the Poiseuille equation is used to establish the flow rate, *Qv*, which is given by [4]:

$$Q_v = \frac{\pi D_n^4 \Delta P}{128\mu L_n} . \quad (9)$$

where μ is the fluid viscosity, D_n the internal diameter and L_n the needle length.

From equations "(4)", "(8)" and "(9)" the thrust force is written under the following form:

$$F_p = \left(P_M + \frac{16\rho Q_v^2}{\pi^2 D_n^4} + \frac{128\mu Q_v L_n}{\pi D_n^4} + \frac{8\rho K_c Q_v^2}{\pi^2 D_n^4} \right)\left(\frac{\pi D_s^2}{4} \right). \quad (10)$$

Fig.3. shows the force evolution according to the fluid flow rate.

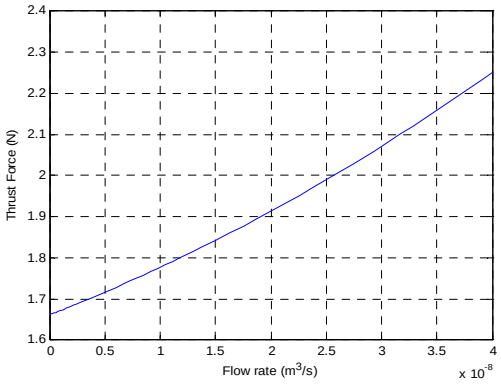

Fig.3. Thrust force evolution according to the fluid flow rate

From this study, it's comes that to be able to ensure perfusions with fluid flow rates of [0.1ml/h 99.9ml/h] or in international system of unit, [2.810^{-11}m^3/s 2.710^{-8}m^3/s], it is necessary that the motorization actuator develops an axial force of maintenance of 2 N. A safety margin of 25% is adopted on the thrust force to avoid unhooking in the event of occlusion or of the pinching. This characteristic will condition

the design of the syringe pump actuator. Knowing that it is necessary to take account of the losses in the actuator in the phase of the design which are due to the transformation of part of the electric power provided by the supply in heat, as well as the ferromagnetic materials subjected to variable flows warm up because of the eddy currents and hysteresis [5]. These losses can entrained a rise in the temperature in the various parts of the actuator, consequently an excessive heating can bring to the deterioration of insulating materials of the windings stator, thus causing the reduction of normal operation of the actuator [5], [6].

3.2. Thermal model

The thermal modelling of the actuator is done under two assumptions. They are justified in this case due to the low power of the system [7]:

- The windings are surrounded air, and the heat is evacuated only by means of natural convection;
- Phase winding's heating is only due to its own Joule losses and Iron losses.

Considering these assumptions, the stator thermal model for each phase is [7], [8]:

$$\Delta T = \frac{\rho_{cu}\delta^2 V_{cu}}{\alpha S_{con}} . \quad (11)$$

where δ is the surface current density, V_{cu} the volume of the coil conductors, ρ_{cu} the copper resistivity, α the convection coefficient ($12Wm^{-2}\,K^{-1}$ for natural convection) and S_{con} the coils surface where convection takes place.

The thermal model is used to limit the stator current. The conductors insulation has a maximal allowable temperature $T_{max}=135°C$ and this value sets the maximal over-temperature $\Delta T_{\max}$ of the wires. Using "(11)", the limiting surface current density producing this over-temperature is given by:

$$\delta = \sqrt{\frac{\Delta T_{\max}\alpha S_{con}}{\rho_{cu}V_{cu}}} . \quad (12)$$

4. Geometrical Dimensions

The electromagnetic structure, on which the optimal design approach is tested, is a linear tubular switched reluctance actuator. It presents four statoric phases and toothed stator and plunger structures with the same tooth and slot widths ($a=b$) [9]. Non-magnetic separations are set between the statoric phases so that only one statoric phase can be aligned with plunger teeth when it is supplied [10].

With the assumption that the actuator is perfectly axi-symmetric and that the statoric phases are not magnetically coupled [11]; the construction of the actuator can then be obtained by assembly of elementary modules shown in the axial plane on Fig.4.

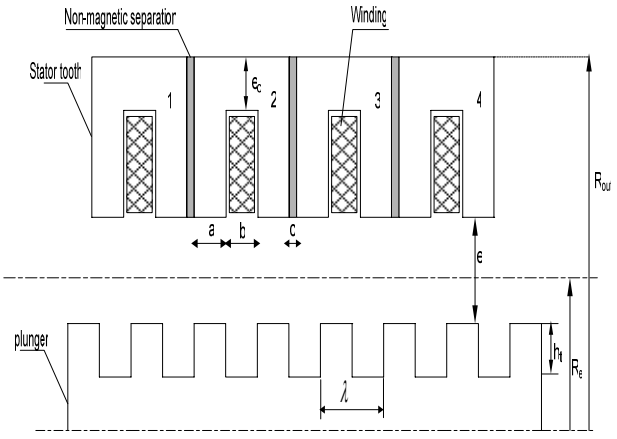

Fig. 4. Half cross-section of the four phase actuator

The geometry of this actuator is characterized by the pole pitch λ (λ=4 mm) given by [11]:

$$a + b = \lambda \ . \tag{13}$$

The stator tooth and slot width is, respectively a and b, are equal.

The static electromagnetic force developed by the actuator is written under the following form [11], [12]:

$$F(z) = \frac{\pi \mu_0 R_e (Ni)^2}{2e} . \tag{14}$$

where R_e is the air-gap radius, Ni the ampere turns and μ_0 the air magnetic permeability.

The optimal air gap radius is given by [11]:

$$R_e = \left(\sqrt{2} - 1\right)\left(R_{out} - e_c\right) . \tag{15}$$

The supply current is written under the following form:

$$i = \delta . S_c \ . \tag{16}$$

where Sc is the conductor section.

The conductor section can be expressed by [11]:

$$S_c = \frac{k_{bob}.S_{bob}}{N} = \frac{k_{bob}.b.\left(\left(R_{out} - e_c\right) - \left(R_e + \frac{e}{2}\right)\right)}{N}. \quad (17)$$

where K_{bob} is the winding factor, S_{bob} the winding section, N the whorl numbes, e_c the yoke thickness, e the air gap thickness and R_{out} the external radius.

From equations "(12)", "(14)", "(16)" and "(17)" the static electromagnetic force expression is given by:

$$F(z) = \frac{\pi\mu_0 R_e \alpha \Delta T S_{th}}{2e\rho_{cu} V_{cu}} k_{bob}^2 b^2 \left(\left(R_{out} - e_c\right) - \left(R_e + \frac{e}{2}\right)\right)^2. \quad (18)$$

This expression will be used for the determination of the geometrical parameters of the actuator. The air gap thickness e is fixed to 0.1 mm and the yoke thickness e_c to 3 mm.

According to Fig. 5. for the static electromagnetic force of 2.5 N, the external radius R_{out} of actuator must be equal 42 mm.

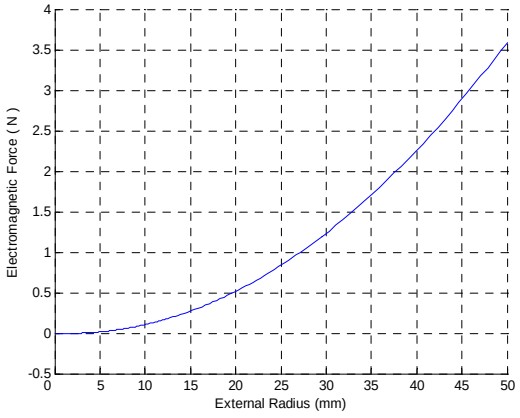

Fig. 5. Variation of the thrust force according to the external radius

Geometrical dimensions of the step actuator are gathered in Table 1.

Table 1. Geometric parameters of the actuator

Parameter		**Value [mm]**
Pole pitch	λ	4
Elementary step	λ_p	1
Stator tooth	a	2
Slot width	b	2
Non-magnetic separation thickness	c	1
Yoke	e_c	3
Air-gap radius	R_e	16.15
Plunger tooth	h_t	2
Air gap thickness	e	0.1
External radius	R_{out}	42

The dynamic electromagnetic force is created starting from the air-gap reluctance variation. Indeed, each change of the plunger position generates a force computed from the following expression [11]:

$$F(i,z) = \frac{1}{2} \sum_{air-gap} (Ni)^2 \frac{\Delta \Re(z)}{\Delta z}. \qquad (19)$$

The air-gap reluctance as well as the corresponding electromagnetic force are computed for different plunger positions with tooth shift percentages varying from 0%, where plunger and stator teeth are aligned, to 50%, Fig.6.

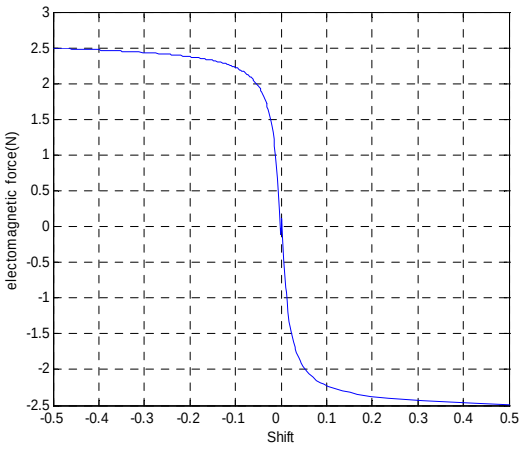

Fig. 6. Evolution of the electromagnetic force according to the shift

5. Validation of the Protype Design using the Finite Element Method

The finite element (FE) method is a powerful numerical method for the resolution of the Maxwell's partial differential equations. It is widely used for the numerical analysis of electrical machines. In general, obtaining a solvable finite element model requires several simplifications of the original physical system, in order to reduce its complexity.

The magnetodynamic behavior of the linear tubular step actuator is governed by equation "(18)" [13]:

$$\frac{\partial}{\partial r}\left[\frac{\upsilon}{r}\frac{\partial(rA)}{\partial r}\right]+\frac{\partial}{\partial z}\left[\frac{\upsilon}{r}\frac{\partial(rA)}{\partial z}\right]=J\ . \qquad (20)$$

where A is the magnetic vector potential, J the current density vector, υ magnetic reluctivity, ∂z the longitudinal elementary displacement.

In addition, the mesh is chosen dense and regular, in the air gap and let free outside. Figure 7 shows the mesh structure under "Opera-2d" commercial software.

Magneto-static simulations are achieved is done in order to determine the thrust force evolutions versus plunger positions.

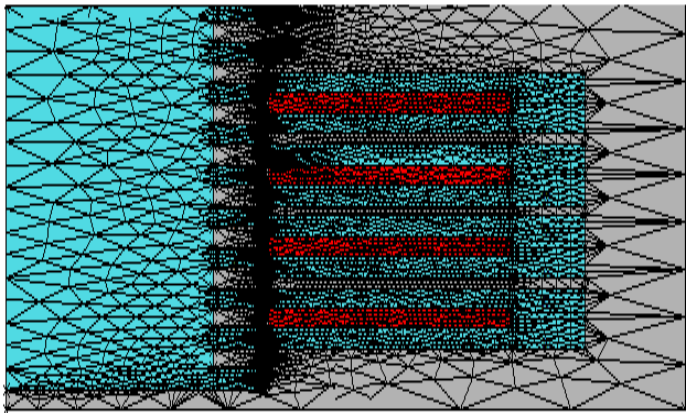

Fig.7. Finite element mesh of the studied actuator

Fig.8. shows the obtained results relative to the magnetic flux distribution taking into account the non-linearity of the material, when the stator first phase and the plunger teeth are aligned. The actuator first phase is supplied by the 0.25 A.

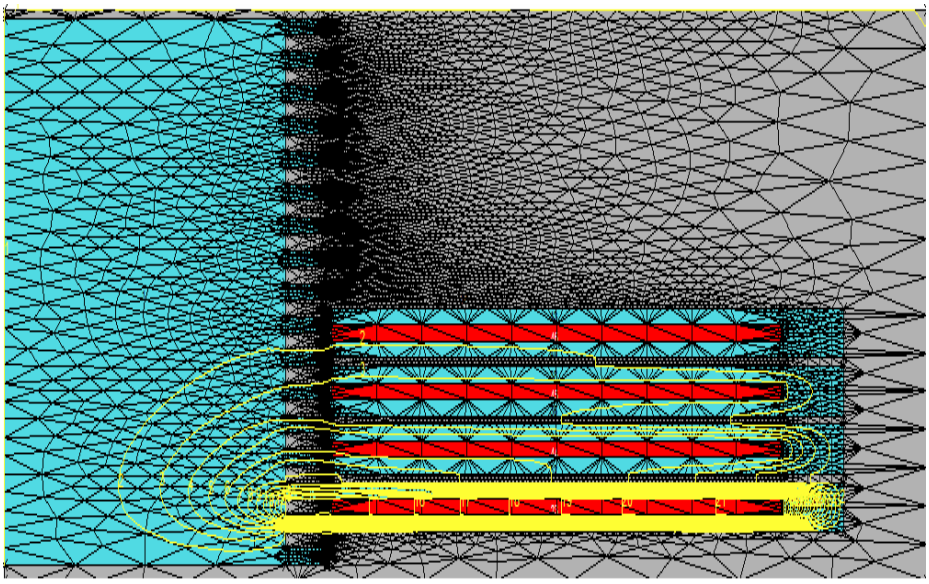

Fig.8. Induction distribution in the magnetic circuit of the first phase

Fig.8. show magnetic leakages through the one supplied phases of the actuator in spite of the existence of non-magnetic separations between the phases. Thus, parasitic forces reducing the total force developed by the step actuator is produced [14], [15].

5.1. Thrust Force Computation

The thrust force developed by the actuator plunger is deduced from the following expression of Maxwell stress tensor [16], [17], [18], [19]:

$$\frac{d\vec{F}}{dS} = -\frac{\mu_0}{2} H^2 \vec{u_r} + \mu_0 \left(\vec{H}\vec{u_r}\right)\vec{H} \,. \qquad (21)$$

where dS is an elementary surface inside the air gap, $\vec{u_r}$ its normal unit vector, H the magnetic field intensity, μ_0 the air magnetic permeability and dS is an R radius cylindrical surface-element situated inside the air-gap.

Inside the air gap region, the magnetic induction vector is described by the following expression [10]:

$$\vec{B} = B_r \vec{u_r} + B_z \vec{u_z} = \mu_0 \vec{H} \,. \qquad (22)$$

where B_z is the axial component of the magnetic flux density and B_r the radial component.

In order to compute the resulting force, the elementary force must be integrated on a cylinder placed within the air gap; its differential surface dS is given by:

$$dS = Rd\theta dz \ . \tag{23}$$

where R is the cylinder radius, dz the longitudinal elementary displacement and $d\theta$ an angle variation.

Thus, the z component of the magnetic pressure is given by:

$$\left(\frac{dF}{dS}\right)_z = \frac{1}{\mu_0} B_r B_z \ . \tag{24}$$

The axial component of the propulsive force can be expressed by [11], [17]:

$$F(z) = \frac{2.\pi}{\mu_0} \int R B_r B_z dz \ . \tag{25}$$

The thrust force is computed for different plunger positions with a tooth shift percentages varying from 0%, where plunger and stator teeth are aligned, to 60%. The corresponding force is given on Fig. 9. The maximal magnitude of the force, which the actuator can develop, is of 2.3 N for a supply current of 0.25 A. This result validates the dimensioning assumptions used by the analytical model.

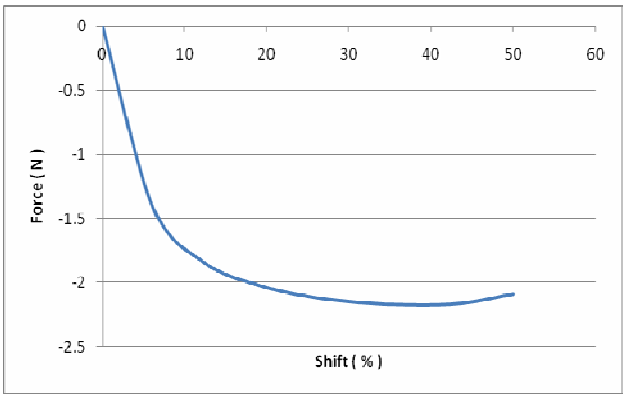

Fig.9. Force characteristic from finite element simulations

5.2. Thrust Force Computation

The characteristics statics of the actuator, Fig.6, Fig.9, show a good concordance between the results obtained from the method of the reluctance network and the finite element method for calculation of force but with a relative error overall lower than 10%. This precision is acceptable insofar as this model worked out for the dimensioning of the actuator.

The resolution of the magnetostatic problem for the linear actuator lasted with one processor Pentium IV-2.2GHz, on an electric quarter of cycle requires approximately 6 hour for a value of current given. So, for this actuator range of very weak thickness of the air-gap, the method of the network reluctance seems to be sturdier and less expensive in simulation time for force calculation.

6. Conclusion

The work presented in this paper describes the stages of a linear step actuator design. This actuator is used for the motorization of a syringe pump. An analytical model for dimensioning of a tubular incremental linear actuator was presented. The equations mathematics characterizing the model describe the geometrical structure and the principal physical properties of the system, by taking account of the thermal stresses, of loads and magnetic.

The study into magnetostatic nonlinear by the software of computer-aided design "Opera-2d" validated by opposite way of the results obtained by the analytical method.

The elaborate analytical model is completely parameterized; it can be applied to dimension other linear tubular step actuator.

References

1. Cazlaa, J.B., Fougere, S., Barrier, G. : Les appareils é1ectriques de perfusion: Annalesfrançais d'anesthésie de reanimation, Vol.13, (1994) 350–359
2. Kahwati, C. : Cas concrets corrigés: calculs de dose : Edition Lamarre, Paris (2001)
3. Chen, X.B., Schoenau, G., Zhang, W. J.: Modelling of time-pressure fluid dispensing process, IEEE Transactions Electronics Packaging Manufacturing, Vol. 23, October (2000), 300–305
4. Chen, X.B.: Modelling and off-line control of fluid dispensing for electronics packaging, Doctorate Thesis. Dissertation, University of Saskatchewan, Saskatoon, Canada (2002)
5. Mayé, P. : Moteurs électriques pour la robotique, Edition Dunod, Paris(2000)
6. Regnier, J. : Conception de systèmes hétérogènes en génie électrique par optimisation évolutionnaire multicritère, Doctorate Thesis, Institut Nationale Polytechnique de Toulouse (2003)
7. Merzaghi, S., Stefanini, I., Markovic, M., Perriard, Y.: Optimization of biomedical actuator for implantable continuous glucose monitoring, IEEE Transactions Electronics Packaging Manufacturing, Vol. 23, (2007) 869–874

8. Ahmed, H.B., Multon, B., Cavarec, P. E.: Actionneurs linéaires directs et indirects performances limites, Journal Club EEA, University Cergy-Pontoise (2003)
9. El Amraoui, L., Gillon, F., Brochet, P., Benrejeb, M.: Design of a linear tubular step motor, Electromotion'01, 4th International Symposium on Advanced Electromechanical Motion Systems, vol. 1, Bologna (2001), 223-228
10. El Amraoui, L., Gillon, F., Brochet, P., Benrejeb, M.: Méthodes de calcul par éléments finis de la force de poussée dans un vérin électrique, Deuxièmes Journées Scientifiques des Jeunes Chercheurs en Génie Electrique et Informatique, Hammamet (2002)
11. EL Amraoui, L.: Conception Electromagnétique d'une Gamme d'Actionneurs Linéaires Tubulaires à Réluctance Variable, Doctorate Thesis, Ecole Centrale de Lille (2002)
12. El Amraoui, L., Gillon, F., Castelain, A., Brochet, P., Benrejeb, M.: Exprimental validation of a linear tubular actuator design, 15th International Conference on Electrical Machines ICEM02, Bruges (2002)
13. Reece, A. B. J., T. Preston, W.: Finite Element Method in Electrical Power Engineering, Edition Oxford University Press (2000)
14. El Amraoui, L., Gillon, F., Brochet, P., Benrejeb, M.: Exploitation de la méthode des éléments finis pour un positionnement en micropas d'un moteur pas à pas linéaire tubulaire, CIFA'2002, Conférence Internationale Francophone d'Automatique, Nantes (2002)
15. El Amraoui, L., Gillon, F., Brochet, P., Benrejeb, M.: performance estimation of linear tubular actuators, the 17th International Conference on Magnetically Levitated Systems and Linear Drives, Lausanne (2002)
16. Nathan, I., Joao, P.A.B.: Electromagnetics and Calculation of Fields, Springer-Verlag, New York (1992)
17. El Amraoui, L., Gillon, F., Brochet, P., Benrejeb, M.: Influence du taux de distorsion du maillage sur le calcul de force d'un vérin électrique, deuxième Conférence International JTEA'02, Sousse (2002)
18. Hu, G.: Analysis of eddy currents in a permanent magnet tubular slotless motor housing du to motion, ICEM02, 15th International Conference on Electrical Machines, Bruges (2002)
19. Binns, K.J., Lawrenson, P.J., Towbridge, C.W.:The analytical and numerical solution of electrical and magnetic fields, Edition British Library Cataloguing in Publication Data, England (1992)